ACS Photonics

Article

Cite This: ACS Photonics XXXX, XXX, XXX−XXX

pubs.acs.org/journal/apchd5

Ultrafast Dynamics of Hot Electrons in Nanostructures: Distinguishing the Influence on Interband and Plasmon Resonances

Yi Wang,[†] Haotian Shi,[†] Lang Shen,[‡] Yu Wang,[‡] Stephen B. Cronin,[§] and Jahan M. Dawlaty*[,†]

[†]Department of Chemistry, [‡]Department of Materials Science, and [§]Department of Electrical Engineering, University of Southern California, Los Angeles, California 90089, United States

Supporting Information

ABSTRACT: It is often necessary to distinguish between the plasmon oscillations arising from confinement in nanostructures and interband transitions characteristic of the bulk. Grating nanostructures are an ideal platform to achieve this goal, since they provide nanoscale confinement in one direction while maintaining macroscopic properties in the other. It is thereby possible to distinguish between confined plasmons and interband transitions by the choice of polarization of the pump and the probe pulses. Here, we report transient absorption (TA) experiments on gold gratings with a 500 nm period pumped with a short pulse centered at 680 nm, reasonably far from the plasmon resonance. The ensuing dynamics of the hot electrons generated by the pump are monitored by broad band visible probe pulses polarized both parallel and perpendicular to the grating lines. We observe a significant difference in the spectral response of the two probe polarizations, while the temporal responses are quite similar. Furthermore, the response of gold nano-gratings qualitatively does not depend on the pump polarization. These results indicate that, regardless of polarization, the pump creates hot electrons in the metal that influence both interband and confined plasmon absorptions. The time-scales of the TA signal, therefore, is indicative of the cooling of the hot electrons as they equilibrate with the lattice. Furthermore, we performed similar experiments on TiO_2-covered gratings and found that it is consistent with the previous work on electron injection into TiO_2, with a response that depends on the pump polarization. These results provide a clearer understanding of the interplay between interband and confined plasmons in photoexcited metal nanostructures.

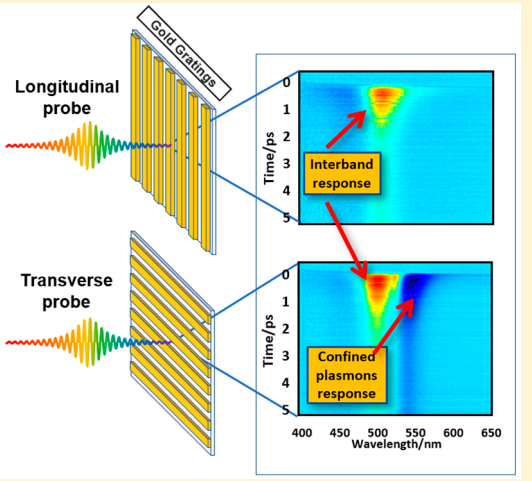

KEYWORDS: *gold grating, local surface plasmon resonance (LSPR), transient absorption spectroscopy, hot electron, interband transition*

Downloaded via UNIV OF SOUTHERN CALIFORNIA on September 16, 2019 at 22:36:36 (UTC).
See https://pubs.acs.org/sharingguidelines for options on how to legitimately share published articles.

Plasmons are the collective oscillations of free electrons in metals.[1,2] In gold, electrons in the 6s band near the Fermi level mainly contribute to the plasmon oscillation.[3−5] Surface plasmons in metals correspond to excitations resulting from the interaction of electromagnetic fields at the boundary of metals and dielectrics.[6] The local surface plasmon resonance (LSPR) in metal nanostructures arises from confinement of surface plasmons when the size of the particle is much smaller than the wavelength of light. This strong confinement of the electromagnetic field in subwavelength-sized nanoparticles has led to various applications, including biomedical sensing,[7−10] optical spectroscopy,[911−15] surface catalysis,[2,16−18] and energy conversion devices.[19−21] The local surface plasmon resonance of gold nanostructures lies within the visible range of the electromagnetic spectrum, making it particularly useful for these applications. Semiconductor-coated metal nanostructures have also shown great potential as novel photocatalysts.[2,22] Many of these studies have shown that hot electrons excited via the local surface plasmon resonance can transfer from below the Fermi level in gold into the conduction band of TiO_2 by overcoming the Schottky barrier at the interface.[5,20,23−26] In this case, the semiconductor−metal interface serves to separate the photoexcited electrons and holes, which is advantageous for energy conversion applications.[27−29]

Ultrafast transient absorption (TA) spectroscopy has been successfully used to characterize the plasmon resonant properties of gold nanoparticles of various sizes and geometries.[16,30−35] However, in most of these works it is difficult to distinguish between the dynamics of confined plasmon resonances and that of the gold interband transitions. The interband transitions in gold appear as a broad peak around 500 nm, which is often attributed to the 5d to 6s interband transition and its ground state bleach. These ultrafast time-resolved studies have shown photoexcited decay on the time scale of 1−2 ps. Della and co-worker reported transient-transmission spectrum of 30 nm gold thin film. Interband transition at 503 nm was observed and the time-scale dynamics

Received: May 31, 2019
Published: August 19, 2019

© XXXX American Chemical Society

DOI: 10.1021/acsphotonics.9b00793
ACS Photonics XXXX, XXX, XXX−XXX

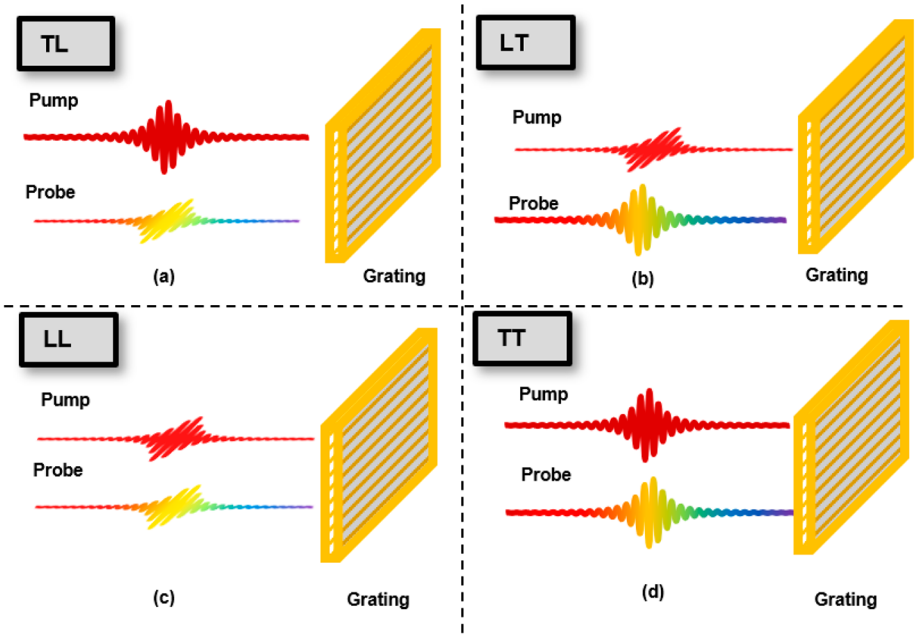

Figure 1. Four experimental configurations arranged according to polarization angles with respect to the gratings: (a) LL (pump longitudinal, probe longitudinal), (b) LT (pump longitudinal, probe transverse), (c) TT (pump transverse, probe transverse), and (d) TL (pump transverse, probe longitudinal).

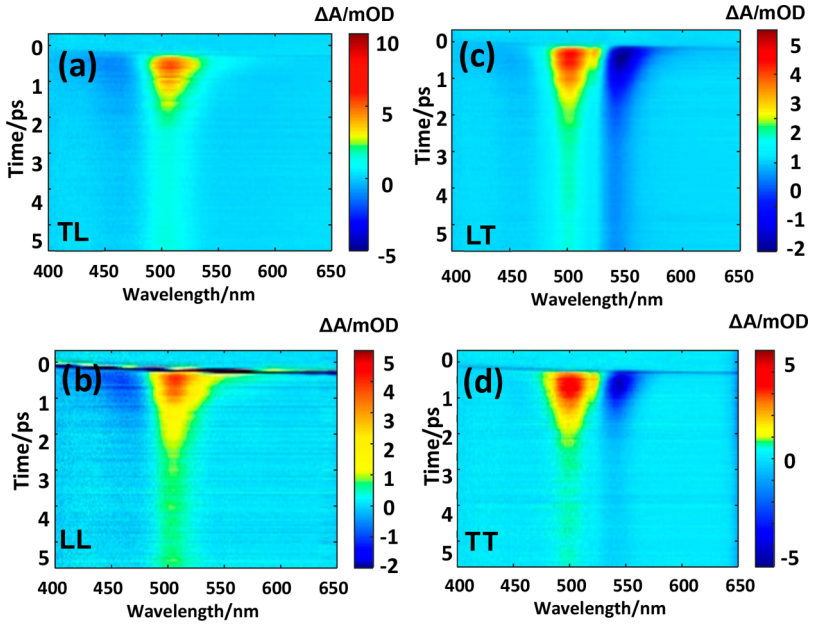

Figure 2. Transient absorption data for bare gold gratings in the polarization configurations described in Figure 1: (a) TL (pump transverse, probe longitudinal), (b) LL (pump longitudinal, probe longitudinal), (c) LT (pump longitudinal, probe transverse), and (d) TT (pump transverse, probe transverse). In (a) and (b) only transient changes in interband absorption (around 510 nm) is observed. In contrast, in (c) and (d), plasmon resonance depletion (around 540 nm) is observed in addition to the interband response.

was reported.[35] Aiboushev and co-workers reported both positive and negative modulations of the absorption ($\Delta A/A$), including an interband transition at 2.4 eV (516 nm) and a plasmon resonance at 2.28 eV (543 nm) for gold nanoparticles (20−80 nm diameter) embedded in a TiO_2 film.[30] In most of these previous studies, because of the spherical symmetry of the nanoparticles and/or inhomogeneity of the samples, there was no easy way to distinguish between LSPR excitations and interband transitions. There has been work reported on nanoparticles that are not spherically symmetric. Payne and co-workers reported extinction spectra of 1170 nm × 49 nm gold nanorods, which show a transverse mode extinction peak at 530 nm, while the longitudinal mode peak is red-shifted to 1300 nm.[36] Notably, the diameter of these nanorods are similar to the thickness of the gratings that have been used in this study, making it an interesting comparison to our work. However, these were ensemble measurements of many randomly oriented nanorods deposited on a surface, and the orientations of the nanorods relative to the polarization of light were not strictly defined.

DOI: 10.1021/acsphotonics.9b00793
ACS Photonics XXXX, XXX, XXX−XXX

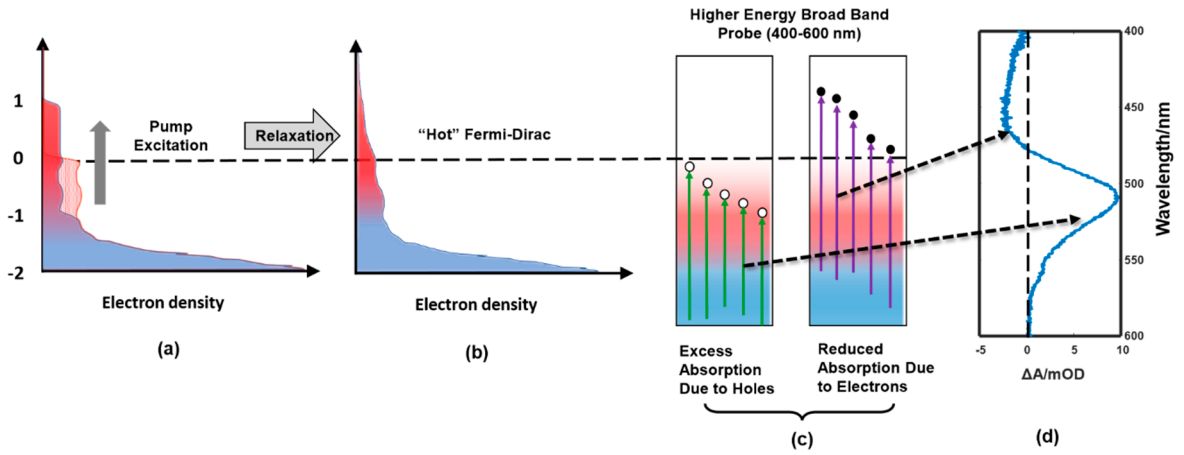

Figure 3. Density of states of gold indicating the features associated with the 6s and 5d bands. (a) The 680 nm pump laser excites electrons from 6s band below the Fermi level to empty states above the Fermi level, generating nonthermal holes and electrons, which thermalize much faster than our time resolution into a new hot Fermi−Dirac distribution (b). (c) The 400−600 nm broadband probe interacts with photoexcited electrons and holes in two ways. Excess absorption is observed around 500 nm due to holes generated below the Fermi level by the pump, corresponding to excited state absorption ($\Delta A/A > 0$). Reduced absorption ($\Delta A/A < 0$) is observed around 470 nm due to absorption blocking by the electrons excited above the Fermi level. (d) Typical transient absorption spectrum of gold and its relation to the optically generated transient electron−hole population.

In order to further distinguish the interband transitions of bulk gold near the Fermi level and the LSPR allowed in nanoscale structures, we designed gold nanoscale gratings to study both bulk-specific phenomena (e.g., interband transitions) and nanospecific phenomena (e.g., LSPR) on the same sample in the same experiment. In the work presented here, we investigate the ultrafast carrier dynamics in gold grating nanostructures with and without TiO_2 coatings. These grating nanostructures provide an ideal platform to study surface plasmon resonance for the following reasons. First, the polarization angle of the incident light with respect to the lines in the gold grating can be changed by simply rotating the gold grating samples and/or waveplates. Since the LSPR cannot be excited when the incident polarization is parallel to the lines in the grating, these grating structures can be used to distinguish the bulk interband absorption and confined plasmon resonances. Here, we measure the pump−probe time-resolved transient absorption spectra of the gold gratings in four different polarization configurations. For clarity of the polarization directions, we have chosen the following terminology. Transverse (T) refers to the polarization of light in which the electric field is perpendicular to the grating lines. Longitudinal (L) refers to the polarization in which the electric field is parallel to the grating lines. The four experimental configurations are as follows (see Figure 1): (1) LL (pump longitudinal, probe longitudinal), (2) LT (pump longitudinal, probe transverse), (3) TT (pump transverse, probe transverse), and (4) TL (pump transverse, probe longitudinal). The bandwidth of the probe (400−700 nm) covers the confined plasmon wavelength, and therefore, the transverse probe is resonant with LSPR, while the longitudinal probe is not. The pump wavelength in all experiments is at 680 nm, which is away from the LSPR. However, as will be shown later, in the TiO_2 covered sample, the polarization of the pump does matter and can influence electron injection into the semiconductor layer. The main purpose of our work is to measure and explain the ultrafast electronic dynamics of the grating nanostructures in these four polarization configurations.

RESULTS AND DISCUSSION

The transient absorption (TA) data for a bare gold grating is presented in Figure 2. Time zero corresponds to the overlap between the pump and probe laser pulses. In all TA measurements, the transient absorption data shows an excited state absorption ($\Delta A/A > 0$) near 510 nm and a reduced absorption wing ($\Delta A/A < 0$) around 450 nm. In Figure 2c,d, when the probe laser is transverse with respect to the grating lines (i.e., resonant with LSPR), the TA data shows additional large depletion (i.e., less absorption) due to the plasmon resonance above 540 nm.

Transient Changes in Interband Transitions. In TA measurements, we have shown excited state absorption corresponding to interband transitions (510 nm) and ground state bleach (450 nm) for all pump polarizations as shown in Figure 2. Comparing all four polarization configurations, we observe that the relative peak intensity, peak positions, and time-resolved dynamics of both the excited state absorption and ground state bleach vary only by a small amount. This result is consistent with our hypothesis that these two features do not depend on the polarization of the pump or probe. In other words, these two peaks have no specific dependence on the nanoconfined direction of the gratings and arise from changes in the interband transitions, as will be discussed below.

The changes in interband transitions can be understood based on the electronic structure of gold, as illustrated in Figure 3a. The electronic density of states of gold is composed of a broad and diffuse 6s band at the Fermi level and a 5d band with a substantially larger density of states ~2 eV below the Fermi level.[37] The 680 nm (1.82 eV) pump pulse creates electron−hole pairs around the Fermi level, primarily within the 6s band, as depicted in Figure 3a,b. The pump excitation creates a non-Fermi−Dirac (nonthermal) distribution, which quickly relaxes (<50 fs) into a hot Fermi−Dirac (thermal) distribution through electron−electron scattering.[38] This process is faster than our time resolution, and therefore we can only observe the influence of the hot thermalized electrons on the optical spectra. The broadband (400−600 nm, 3.10−2.07 eV) probe interrogates this population of electrons and

DOI: 10.1021/acsphotonics.9b00793
ACS Photonics XXXX, XXX, XXX−XXX

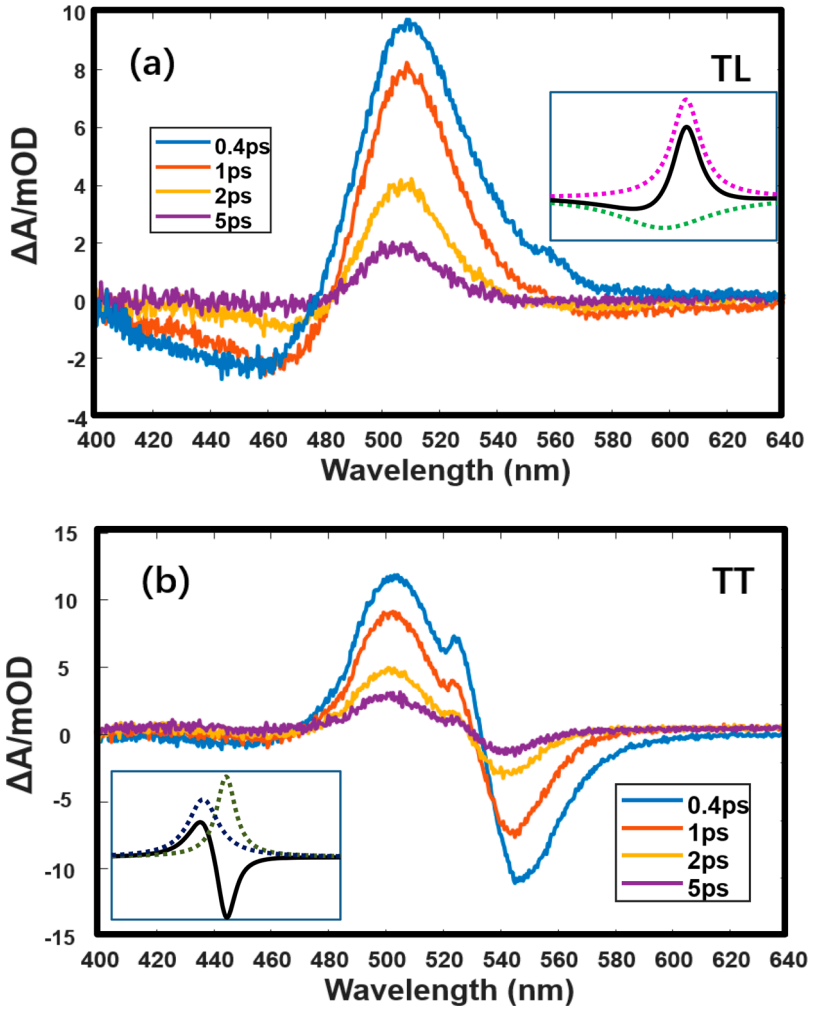

Figure 4. (a) TA spectra for gold gratings pumped at 680 nm, with probe longitudinally polarized with respect to the grating lines. The cartoon illustrates the net TA singal (black solid line) is the result of ground state bleach (green dotted line) above 500 nm adding to excess absorption (pink dotted line) at 520 nm. (b) TA spectra of Au grating with probe transversely polarized with respect to the grating lines. LSPR peak at 545 nm shows up in addition to the interband transition peak. The cartoon illustrates that the unpumped plasmon response (dark green) upon generation of hot carriers is blue-shifted and broadened (dark blue). The TA signal is the result of their subtraction (solid black line).

holes as they further relax through electron−phonon scattering.[39,40] Figure 3c and d schematically show how these photoexcited free carriers result in a modulation of the transient absorption spectrum.

We observe two transient absorption features that arise from interband transitions: a depletion around 480 nm and an absorption peak at 510 nm. The depletion feature corresponds to blocking of excitation of electrons in the 5d band to the 6s band above the Fermi level. The 510 nm positive feature ($\Delta A/A > 0$) is a result of the excited state absorption from the 5d band into the photogenerated holes near the Fermi level. As expected and illustrated in Figure 3, the transient absorption spectrum is the net sum of the excess absorption by the photoexcited holes and the reduced absorption due to blocking by the photoexcited electrons. Although the energy distribution of holes and electrons is strictly symmetric at the Fermi level, the profiles of the depletion peak and the absorption peak are not symmetric. The excess absorption ($\Delta A/A > 0$) corresponds to the transition of electrons from the lower energy band to the hole generated by pump photon, whereas the reduced absorption is transition of electrons from the lower energy band to empty states above the Fermi level. Transitions of electrons to the empty states above the Fermi level have a much wider range than the transitions of electrons to the holes generated by the pump. As a result the excess absorption has a much narrower peak (500−520 nm) than that of the reduced absorption peak (from 450 nm up to over 500 nm) due to the difference in the nature of the two absorption mechanisms. Excess absorption only takes place where the holes are generated by the pump, in our case, 1.8 eV below the Fermi level. For the reduced absorption peak, however, the transition can take place anywhere from the 5d band to just below the Fermi level. Therefore, one can not a priori anticipate the TA signal to be symmetric. The data and the above explanation are consistent with many previous observations in the literature for gold nanoparticles.[30−32,41]

Following the TA spectra in time, we observe that the excess absorption peak is blue-shifted as time progresses, while the reduced absorption peak is red-shifted (see Figure 4a, around 450 nm). This is due the hot Fermi−Dirac distribution cooling off as it dissipates heat into the gold lattice via electron−phonon scattering resulting in the reduction in the signal and narrowing of the hot electron-smearing around the Fermi level.[5]

DOI: 10.1021/acsphotonics.9b00793
ACS Photonics XXXX, XXX, XXX−XXX

Transient Changes in Confined Plasmon Absorption. Figure 2c,d shows the transient changes of the gold gratings when the probe pulse is transverse to the grating lines. In addition to the reduced absorption at 460 nm and excess absorption at 510 nm, a large depletion peak around 540 nmappears in both spectra. The peak at 540 nm is the result of plasmon derived hot electrons. Pump laser produces hot electrons and holes around the Fermi level. The bleach in the LSPR response due to a change in the population of carriers surrounding the Fermi level. The pump wavelength (680 nm) is longer than that of the plasmon resonant mode (540 nm) and, therefore, very likely it does not excite the grating through the LSPR, even for the transverse polarization.

The dimensions of gold gratings are 45 nm thick and 250 nm wide with a 250 nm gap between the lines. The LSPR oscillation is confined by the thickness of the grating lines and corresponds to oscillation of electrons perpendicular to the lines of the grating. This resonant mode can be probed by transversely polarized light with respect to the grating lines. When the probe is longitudinally polarized, however, the electrons oscillate along the surface and are not affected by the confinement. Payne and co-workers reported extinction spectra of 1170 nm × 49 nm gold nanorods.[36] The thickness of the grating used in this work is 45 nm, which has similar confinement to the transverse mode of their nanorods. In their work, the transverse mode was at 580 nm, while the longitudinal mode was in the near IR region. Therefore, it is reasonable to believe that the thickness of the grating will lead to confined LSPR near 545 nm, as seen in our data. Given the differences in the size (49 nm vs 45 nm), geometry (nanorods vs grating lines), and environment (bulk vs deposited on glass) between their work and our gratings, it is justifiable that the LSPR in the gratings would occur at a slightly different wavelength, and very likely blue-shifted.

It has been previously reported in the literature that the LSPR frequency is a function of the electronic temperature.[42] Therefore, it is reasonable to believe that after heating of the electrons with the pump pulse, the LSPR spectrum has shifted and likely broadened. In the differential transient signal (i.e., difference between pumped and unpumped sample) this results in a negative and slightly shifted peak as observed in the Figure 4b. The magnitude of this peak continues to decrease as the hot electrons cool off and transfer energy to the lattice. Importantly, the time-scale of decay of the LSPR signal is similar to that of the interband transitions, which is consistent with the fact that they are both affected by the cooling of the hot electrons. Another important observation is that the LSPR dynamics as measured by the probe is independent of the pump polarization. Since the pump is not resonant with the LSPR, it generates hot electrons for both longitudinal and transverse polarization.

TiO_2-Coated Grating. In order to explore the influence of a different interface other than air, and to identify the possibility of electron injection from the metal to a semiconductor as reported before,[24,43,44] we chose to study the ultrafast dynamics of these grating lines after they were coated with a thin (5 nm) TiO_2 layer. Figure 5 shows the TA spectra of the TiO_2-coated grating. The negative feature indicative of the LSPR dynamics appearing in the transversely polarized probe appears around 560 nm, which is significantly red-shifted compared to a similar feature in the bare grating (540 nm). This is consistent with previous observations that the dielectric constant of the surrounding medium affects the

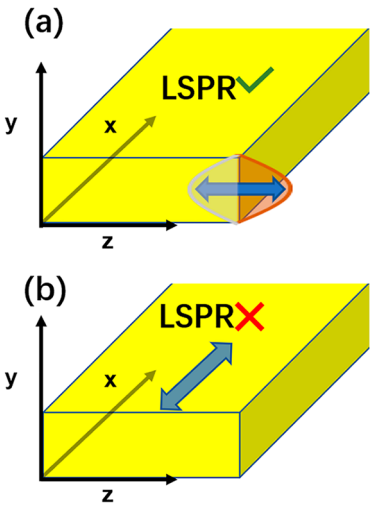

Figure 5. (a) LSPR is activated when the probe is transversely polarized (z-axis), when the LSPR is confined by the thickness of the grating (y-axis). (b) LSPR is not activated when the probe is longitudinally polarized (x-axis), when the LSPR cannot be confined along the grating line (x-axis).

LSPR frequency. Equation 1 expresses the relation between plasmon frequency in metal and the surface plasmon resonance frequency. Here is the dielectric constant correction due to interband transition and the dielectric constant of the surrounding dielectric interface.[45−47]

$$\omega_{sp}^{\ 2} = \frac{\omega_p^{\ 2}}{1 + \epsilon_{ib} + 2\epsilon_m} \quad (1)$$

Based on this, higher dielectric constants (TiO_2 compared to air) are expected to red-shift the LSPR. Another important distinguishing feature of the TiO_2-covered gratings compared to bare gratings is the dependence of the signal on pump polarization. Unlike the bare gratings, in which the LSPR dynamics was independent of the polarization of the pump, in the coated gratings we observe a difference. The LSPR feature appears near ∼560 nm when pumped with transversely polarized light and red-shifted to ∼580 nm when the pump is longitudinally polarized. Ultrafast light-induced electron transfer between a metal and semiconductor has been reported previously,[25,43] due to two mechanisms. The first mechanism is direct charge transfer from the metal to the semiconductor by photon excitation. The second mechanism involves hot electrons created by light that overcome the metal−semiconductor barrier. It is likely that, in our TiO_2-coated gratings, electrons are transferred from gold to the semiconductor layer due to the pump excitation, resulting in manifestly different TA spectra and on pump polarization dependence compared to the bare gratings. It is likely that electron transfer in our case does not occur through excitation of the LSPR, since our pump is lower in energy (680 nm) compared to the LSPR (∼540 nm). Electron injection is expected to increase the dielectric constant of TiO_2 that, according to eq 1, will result in a red shift of the LSPR, as shown in Figure 5c,d. Many previous studies reported that the pump can produce hot electrons, which can overcome the Schottky barrier (0.24 eV) to enable charge transfer from gold into the TiO_2 semiconductor.[47,48] Long and Prezhdo proposed a theoretical model of charge transfer between gold nanoparticles and TiO_2. The electrons in

DOI: 10.1021/acsphotonics.9b00793
ACS Photonics XXXX, XXX, XXX−XXX

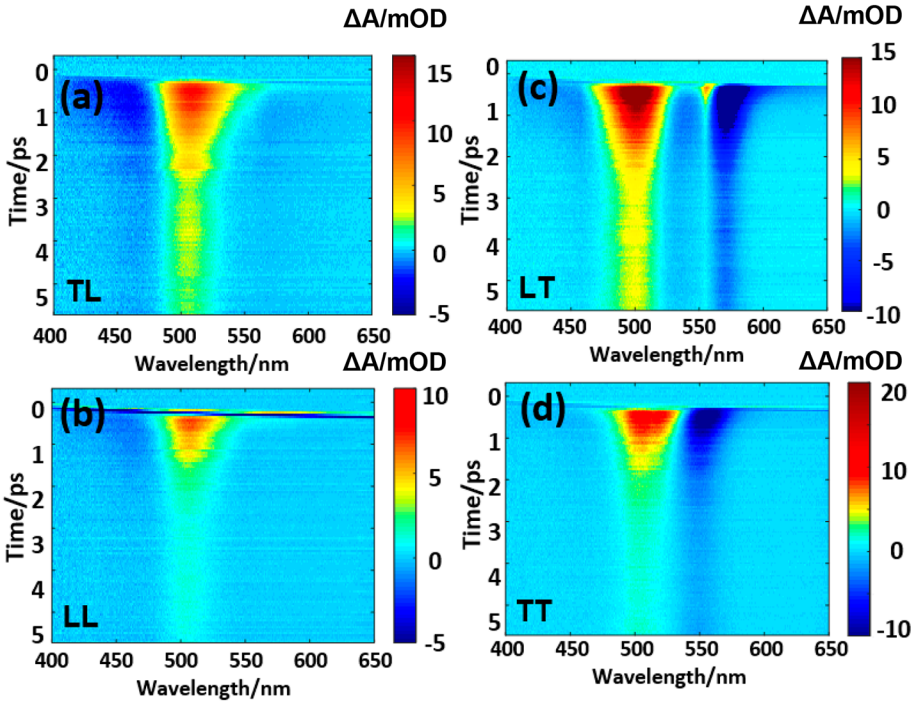

Figure 6. Transient absorption data for TiO_2-coated Au gratings in four basic polarization configurations: (a) TL (pump transverse, probe longitudinal), (b) LL (pump longitudinal, probe longitudinal), (c) LT (pump longitudinal, probe transverse), and (d) TT (pump transverse, probe transverse). Only interband absorption (around 510 nm) is observed in (a) and (b). LSPR depletion (around 560 nm) is observed in (d) and the LSPR red-shifted to 580 nm with pump transversely polarized in (c).

gold transferred into TiO_2 immediately after plasmon excitation due to delocalization of plasma into the TiO_2 layer.[48] However, polarization-dependent studies are scarcely found. Based on the experimental results, we believe more electrons transfer to the conduction band of TiO_2 when the pump is longitudinally polarized than transversely polarized, based on the more redshift observed. We do not have a fundamental mechanism that supports injection of more electrons with the longitudinally polarized pump. At this moment, we believe that the full explanation of electron injection as influenced by the polarization of light is still lacking and needs to be developed in future work.

METHODS

Sample Preparation. In fabricating the grating structure, we pattern 250 nm thick lines in a gold film with a 500 nm period using photolithography and reactive ion etching. The lithography was performed using an ASML deep UV stepper lithography tool. These grating structures were patterned on a transparent BK-7 substrate, which enables transient absorption spectra to be readily obtained. Figure S1 shows a SEM image and a UV−vis spectrum of the gold grating, with plasmon-resonant features around 550 and 760 nm.

Transient Absorption Measurements. Pump pulses were generated by pumping an OPA (OPerA Solo, Coherent) with the output of a 1 kHz Ti:sapphire amplifier (Legend Elite HE+, Coherent). Pump pulses were generated by a doubling stage of the OPA output. A white light continuum probe was prepared by focusing the 800 nm Ti:sapphire output onto a 3 mm thick rotating CaF_2 window after the seed pulse was modulated at 500 Hz using an optical chopper. The polarization of the 800 nm Ti:sapphire output was rotated using waveplate to set the polarization of white light continuum probe either 0°or 90°with respect to the laser table. The pump beam was modulated at 250 Hz. A balanced detection scheme was employed to eliminate noise due to fluctuations in the probe spectrum. The probe arm was focused into the sample and overlapped with the focused pump beam. The reference arm was focused on the sample but not overlapped with the pump beam. The probe beams were detected using a 320 mm focal length spectrometer with 150 g/mm gratings (Horiba iHR320) and a 1340 × 100 CCD array (Princeton Instruments Pixis). Both probe beams were detected on the CCD by displacing their focal planes into the spectrometer. The sample and reference beams were captured by the top half and the bottom half of the CCD, respectively. The signal resulting from the sample beam contains the transient absorption and fluctuations due to the instability of the probe. The signal resulting from the reference beam only contains the fluctuations. The reported transient absorption signals were calculated by subtracting the reference signal from the sample signal. The focal spot diameters for the pump and probe were 140 and 180 μm, respectively. Cross correlations of the pump and probe were collected using the nonresonant response of each sample. The time resolution of each experiment was determined by either the cross correlation (300 fs) or the temporal step size, depending on which was longer.[49,50]

CONCLUSIONS

We measured the transient absorption spectra of gold gratings with and without TiO_2 coatings. The structure of the gold grating, which allows confinement of localized surface plasmons in one direction, enables us to distinguish the dynamics of the interband transitions from the LSPR by the choice of probe polarization. We also demonstrate that the

DOI: 10.1021/acsphotonics.9b00793
ACS Photonics XXXX, XXX, XXX−XXX

pump polarization does not qualitatively influence the transient response of the interband transitions and localized surface plasmons. This indicates that either polarization of the pump produces hot electrons, which in turn affects the transient signal due to both interband and LSPR transitions. Our results on TiO_2-covered gratings, however, show dependence on pump polarization and indicate at possible electron transfer from the metal to the TiO_2 layer. However, the mechanism underlying this polarization dependence of the pump excitation affects this electron transfer process needs further investigation.

■ ASSOCIATED CONTENT

Supporting Information

The Supporting Information is available free of charge on the ACS Publications website at DOI: 10.1021/acsphotonics.9b00793.

SEM image and UV−vis transmission spectrum of a gold gratings (Figure S1). Selected transient absorption spectra extracted from the data shown in Figure 6 (Figure S2). Transient absorption data for gold grating structure with 560 nm pump pulses (Figures S3 and S4) (PDF)

■ AUTHOR INFORMATION

Corresponding Author

*E-mail: dawlaty@usc.edu. Phone: 213-740-9337.

ORCID

Stephen B. Cronin: 0000-0001-7089-6672

Jahan M. Dawlaty: 0000-0001-5218-847X

Notes

The authors declare no competing financial interest.

■ ACKNOWLEDGMENTS

This research was supported by the Army Research Office (ARO) Award No. W911NF-17-1-0325 and NSF CAREER Award (1454467) (Yi W.), the U.S. Department of Energy (DOE), Office of Science, Office of Basic Energy Sciences (BES), under Award DE-SC0019322 (Yu W.), NSF Award No. CBET-1512505 (H.S.), and Air Force Office of Scientific Research (AFOSR) Grant No. FA9550-15-1-0184 (L.S.).

■ REFERENCES

(1) Kino, G. S.; Sundaramurthy, A.; Schuck, P. J.; Fromm, D. P.; Moerner, W. E., Optical field enhancement with plasmon resonant bowtie nanoantennas. In *Surface Plasmon Nanophotonics*; Brongersma, M. L., Kik, P. G., Eds.; Springer Netherlands: Dordrecht, 2007; pp 125−137.

(2) Hou, W.; Cronin, S. B. A review of surface plasmon resonance-enhanced photocatalysis. *Adv. Funct. Mater.* **2013**, *23*, 1612−1619.

(3) Amendola, V.; Pilot, R.; Frasconi, M.; Marago, O. M.; Iati, M. A. Surface plasmon resonance in gold nanoparticles: A review. *J. Phys.: Condens. Matter* **2017**, *29*, 203002.

(4) Eustis, S.; El-Sayed, M. A. Why gold nanoparticles are more precious than pretty gold: Noble metal surface plasmon resonance and its enhancement of the radiative and nonradiative properties of nanocrystals of different shapes. *Chem. Soc. Rev.* **2006**, *35*, 209−217.

(5) Sundararaman, R.; Narang, P.; Jermyn, A. S.; Goddard, W. A., III; Atwater, H. A. Theoretical predictions for hot-carrier generation from surface plasmon decay. *Nat. Commun.* **2014**, *5*, 5788.

(6) Haes, A. J.; Van Duyne, R. P. A unified view of propagating and localized surface plasmon resonance biosensors. *Anal. Bioanal. Chem.* **2004**, *379*, 920−930.

(7) Homola, J.; Yee, S. S.; Gauglitz, G. Surface plasmon resonance sensors: Review. *Sens. Actuators, B* **1999**, *54*, 3−15.

(8) Petryayeva, E.; Krull, U. J. Localized surface plasmon resonance: Nanostructures, bioassays and biosensing—a review. *Anal. Chim. Acta* **2011**, *706*, 8−24.

(9) Willets, K. A.; Van Duyne, R. P. Localized surface plasmon resonance spectroscopy and sensing. *Annu. Rev. Phys. Chem.* **2007**, *58*, 267−97.

(10) Szunerits, S.; Spadavecchia, J.; Boukherroub, R. Surface plasmon resonance: Signal amplification using colloidal gold nanoparticles for enhanced sensitivity. *Rev. Anal. Chem.* **2014**, *33*, 153−164.

(11) Gieseking, R. L.; Ratner, M. A.; Schatz, G. C. Review of plasmon-induced hot-electron dynamics and related sers chemical effects. *Frontiers of Plasmon Enhanced Spectroscopy Volume* **2016**, *1*, 1−22.

(12) Anker, J. N.; Hall, W. P.; Lyandres, O.; Shah, N. C.; Zhao, J.; Van Duyne, R. P., Biosensing with plasmonic nanosensors. In *Nanoscience and Technology: A Collection of Reviews from Nature Journals*; World Scientific, 2010; pp 308−319.

(13) Jackson, J. B.; Halas, N. J. Surface-enhanced raman scattering on tunable plasmonic nanoparticle substrates. *Proc. Natl. Acad. Sci. U. S. A.* **2004**, *101*, 17930−17935.

(14) Sharma, B.; Frontiera, R. R.; Henry, A.-I.; Ringe, E.; Van Duyne, R. P. Sers: Materials, applications, and the future. *Mater. Today* **2012**, *15*, 16−25.

(15) Marimuthu, A.; Zhang, J.; Linic, S. Tuning selectivity in propylene epoxidation by plasmon mediated photo-switching of cu oxidation state. *Science* **2013**, *339*, 1590−1593.

(16) Liu, Z.; Hou, W.; Pavaskar, P.; Aykol, M.; Cronin, S. B. Plasmon resonant enhancement of photocatalytic water splitting under visible illumination. *Nano Lett.* **2011**, *11*, 1111−1116.

(17) Ingram, D. B.; Linic, S. Water splitting on composite plasmonic-metal/semiconductor photoelectrodes: Evidence for selective plasmon-induced formation of charge carriers near the semiconductor surface. *J. Am. Chem. Soc.* **2011**, *133*, 5202−5205.

(18) Christopher, P.; Xin, H.; Linic, S. Visible-light-enhanced catalytic oxidation reactions on plasmonic silver nanostructures. *Nat. Chem.* **2011**, *3*, 467.

(19) Zhong, Y.; Ueno, K.; Mori, Y.; Shi, X.; Oshikiri, T.; Murakoshi, K.; Inoue, H.; Misawa, H. Plasmon-assisted water splitting using two sides of the same srtio3 single-crystal substrate: Conversion of visible light to chemical energy. *Angew. Chem., Int. Ed.* **2014**, *53*, 10350−10354.

(20) Li, J.; Cushing, S. K.; Meng, F.; Senty, T. R.; Bristow, A. D.; Wu, N. Plasmon-induced resonance energy transfer for solar energy conversion. *Nat. Photonics* **2015**, *9*, 601.

(21) Lee, M.-K.; Kim, T. G.; Kim, W.; Sung, Y.-M. Surface plasmon resonance (spr) electron and energy transfer in noble metal- zinc oxide composite nanocrystals. *J. Phys. Chem. C* **2008**, *112*, 10079−10082.

(22) Ingram, D. B.; Linic, S. Water splitting on composite plasmonic-metal/semiconductor photoelectrodes: Evidence for selective plasmon-induced formation of charge carriers near the semiconductor surface. *J. Am. Chem. Soc.* **2011**, *133*, 5202−5205.

(23) Yang, Y.; Lian, T. Multiple exciton dissociation and hot electron extraction by ultrafast interfacial electron transfer from pbs qds. *Coord. Chem. Rev.* **2014**, *263−264*, 229−238.

(24) Wu, K.; Rodriguez-Cordoba, W. E.; Yang, Y.; Lian, T. Plasmon-induced hot electron transfer from the au tip to cds rod in cds-au nanoheterostructures. *Nano Lett.* **2013**, *13*, 5255−63.

(25) Furube, A.; Du, L.; Hara, K.; Katoh, R.; Tachiya, M. Ultrafast plasmon-induced electron transfer from gold nanodots into tio2 nanoparticles. *J. Am. Chem. Soc.* **2007**, *129*, 14852−14853.

(26) Zhang, T.; Su, D.; Li, R.-Z.; Wang, S.-J.; Shan, F.; Xu, J.-J.; Zhang, X.-Y. Plasmonic nanostructures for electronic designs of photovoltaic devices: Plasmonic hot-carrier photovoltaic architectures and plasmonic electrode structures. *J. Photonics Energy* **2016**, *6*, 042504.

DOI: 10.1021/acsphotonics.9b00793
ACS Photonics XXXX, XXX, XXX−XXX

(27) Halas, N. J.; Lal, S.; Chang, W.-S.; Link, S.; Nordlander, P. Plasmons in strongly coupled metallic nanostructures. *Chem. Rev.* **2011**, *111*, 3913−3961.
(28) Andrew, P.; Barnes, W. Energy transfer across a metal film mediated by surface plasmon polaritons. *Science* **2004**, *306*, 1002−1005.
(29) Tagliabue, G.; Eghlidi, H.; Poulikakos, D. Facile multifunctional plasmonic sunlight harvesting with tapered triangle nanopatterning of thin films. *Nanoscale* **2013**, *5*, 9957−9962.
(30) Aiboushev, A.; Gostev, F.; Shelaev, I.; Kostrov, A.; Kanaev, A.; Museur, L.; Traore, M.; Sarkisov, O.; Nadtochenko, V. Spectral properties of the surface plasmon resonance and electron injection from gold nanoparticles to tio2 mesoporous film: Femtosecond study. *Photochem. Photobiol. Sci.* **2013**, *12*, 631−7.
(31) Karam, T. E.; Khoury, R. A.; Haber, L. H. Excited-state dynamics of size-dependent colloidal tio2-au nanocomposites. *J. Chem. Phys.* **2016**, *144*, 124704.
(32) Zhang, X.; Huang, C.; Wang, M.; Huang, P.; He, X.; Wei, Z. Transient localized surface plasmon induced by femtosecond interband excitation in gold nanoparticles. *Sci. Rep.* **2018**, *8*, 10499.
(33) Ahmadi, T. S.; Logunov, S. L.; El-Sayed, M. A. Picosecond dynamics of colloidal gold nanoparticles. *J. Phys. Chem.* **1996**, *100*, 8053−8056.
(34) Logunov, S.; Ahmadi, T.; El-Sayed, M.; Khoury, J.; Whetten, R. Electron dynamics of passivated gold nanocrystals probed by subpicosecond transient absorption spectroscopy. *J. Phys. Chem. B* **1997**, *101*, 3713−3719.
(35) Della Valle, G.; Conforti, M.; Longhi, S.; Cerullo, G.; Brida, D. Real-time optical mapping of the dynamics of nonthermal electrons in thin gold films. *Phys. Rev. B: Condens. Matter Mater. Phys.* **2012**, *86*, 155139.
(36) Payne, E. K.; Shuford, K. L.; Park, S.; Schatz, G. C.; Mirkin, C. A. Multipole plasmon resonances in gold nanorods. *J. Phys. Chem. B* **2006**, *110*, 2150−2154.
(37) Yang, L. M.; Dornfeld, M.; Frauenheim, T.; Ganz, E. Glitter in a 2d monolayer. *Phys. Chem. Chem. Phys.* **2015**, *17*, 26036−42.
(38) Link, S.; Burda, C.; Mohamed, M.; Nikoobakht, B.; El-Sayed, M. Femtosecond transient-absorption dynamics of colloidal gold nanorods: Shape independence of the electron-phonon relaxation time. *Phys. Rev. B: Condens. Matter Mater. Phys.* **2000**, *61*, 6086.
(39) Dulkeith, E.; Niedereichholz, T.; Klar, T.; Feldmann, J.; Von Plessen, G.; Gittins, D.; Mayya, K.; Caruso, F. Plasmon emission in photoexcited gold nanoparticles. *Phys. Rev. B: Condens. Matter Mater. Phys.* **2004**, *70*, 205424.
(40) Hodak, J. H.; Henglein, A.; Hartland, G. V. Size dependent properties of au particles: Coherent excitation and dephasing of acoustic vibrational modes. *J. Chem. Phys.* **1999**, *111*, 8613−8621.
(41) Hashimoto, S.; Katayama, T.; Setoura, K.; Strasser, M.; Uwada, T.; Miyasaka, H. Laser-driven phase transitions in aqueous colloidal gold nanoparticles under high pressure: Picosecond pump-probe study. *Phys. Chem. Chem. Phys.* **2016**, *18*, 4994−5004.
(42) Yeshchenko, O. A.; Bondarchuk, I. S.; Gurin, V. S.; Dmitruk, I. M.; Kotko, A. V. Temperature dependence of the surface plasmon resonance in gold nanoparticles. *Surf. Sci.* **2013**, *608*, 275−281.
(43) Wu, K.; Chen, J.; McBride, J. R.; Lian, T. Efficient hot-electron transfer by a plasmon-induced interfacial charge-transfer transition. *Science* **2015**, *349*, 632−635.
(44) Primo, A.; Corma, A.; Garcia, H. Titania supported gold nanoparticles as photocatalyst. *Phys. Chem. Chem. Phys.* **2011**, *13*, 886−910.
(45) Hartland, G. V. Optical studies of dynamics in noble metal nanostructures. *Chem. Rev.* **2011**, *111*, 3858−3887.
(46) Link, S.; Burda, C.; Wang, Z. L.; El-Sayed, M. A. Electron dynamics in gold and gold−silver alloy nanoparticles: The influence of a nonequilibrium electron distribution and the size dependence of the electron−phonon relaxation. *J. Chem. Phys.* **1999**, *111*, 1255−1264.
(47) Tang, H.; Prasad, K.; Sanjines, R.; Schmid, P.; Levy, F. Electrical and optical properties of tio2 anatase thin films. *J. Appl. Phys.* **1994**, *75*, 2042−2047.
(48) Long, R.; Prezhdo, O. V. Instantaneous generation of charge-separated state on tio2 surface sensitized with plasmonic nanoparticles. *J. Am. Chem. Soc.* **2014**, *136*, 4343−4354.
(49) Hunt, J. R.; Dawlaty, J. M. Photodriven deprotonation of alcohols by a quinoline photobase. *J. Phys. Chem. A* **2018**, *122*, 7931−7940.
(50) Driscoll, E. W.; Hunt, J. R.; Dawlaty, J. M. Proton capture dynamics in quinoline photobases: Substituent effect and involvement of triplet states. *J. Phys. Chem. A* **2017**, *121*, 7099−7107.

DOI: 10.1021/acsphotonics.9b00793
ACS Photonics XXXX, XXX, XXX−XXX